The range of accretion rates estimated from Eq. 1, 30 to 60 $M_\odot$ year$^{-1}$, is found to be close to the galaxy's SFR of ~$33^{+40}_{-11}$ $M_\odot$ year$^{-1}$. This is in agreement with the simplest arguments for galaxy growth via self-regulation (24, 25) and from numerical simulations (4, 6). Furthermore, for this galaxy's halo mass, $M_h \sim 4 \times 10^{11}$ $M_\odot$ (determined from its rotation curve), this value of $M_{in}$ corresponds to an accretion efficiency ε of ~100% [where ε is defined as the ratio of the observed and maximum expected baryonic accretion rates, namely $\varepsilon \equiv M_{in}/(f_B \dot{M}_h)$, where $f_B$ is the universal baryonic fraction and $\dot{M}_h$ is the halo growth rate (26, 27)].

Our study shows the potential of the technique of using background quasars passing near galaxies to further understand the process of gas accretion in galaxies, which is complementary to other recent studies (28–30). Our observations, which are merely consistent with cold accretion, provide key evidence important to consider against hydrodynamical simulations.

### References and Notes

1. E. Daddi et al., Astrophys. J. 713, 686 (2010).
2. R. Genzel et al., Mon. Not. R. Astron. Soc. 407, 2091 (2010).
3. D. Kereš, N. Katz, D. H. Weinberg, R. Davé, Mon. Not. R. Astron. Soc. 363, 2 (2005).
4. C.-A. Faucher-Giguère, D. Kereš, C.-P. Ma, Mon. Not. R. Astron. Soc. 417, 2982 (2011).
5. F. van de Voort et al., Mon. Not. R. Astron. Soc. 414, 2458 (2011).
6. A. Dekel et al., Nature 457, 451 (2009).
7. S. D. M. White, C. S. Frenk, Astrophys. J. 379, 52 (1991).
8. Y. Birnboim, A. Dekel, Mon. Not. R. Astron. Soc. 345, 349 (2003).
9. K. R. Stewart et al., Astrophys. J. 738, 39 (2011).
10. S. Shen et al., Astrophys. J. 765, 89 (2013).
11. K. R. Stewart et al., Astrophys. J. 735, L1 (2011).
12. M. Fumagalli et al., Mon. Not. R. Astron. Soc. 418, 1796 (2011).
13. T. Goerdt, A. Dekel, A. Sternberg, O. Gnat, D. Ceverino, Mon. Not. R. Astron. Soc. 424, 2292 (2012).
14. S. Lopez, D. Reimers, S. D'Odorico, J. X. Prochaska, Astron. Astrophys. 385, 778 (2002).
15. SINFONI is the near-infrared integral field spectrograph at one of the Very Large Telescopes (VLTs) of the European Southern Observatory (ESO).
16. N. Bouché et al., Mon. Not. R. Astron. Soc. 419, 2 (2012).
17. See supplementary materials on Science Online.
18. N. M. Förster Schreiber et al., Astrophys. J. 706, 1364 (2009).
19. T. M. Tripp et al., Science 334, 952 (2011).
20. R. Bordoloi et al., Astrophys. J. 743, 10 (2011).
21. N. Bouché et al., Mon. Not. R. Astron. Soc. 426, 801 (2012).
22. G. Kacprzak, C. W. Churchill, N. M. Nielsen, Astrophys. J. 760, L7 (2012).
23. G. Vladilo et al., Astron. Astrophys. 454, 151 (2006).
24. A. A. Dutton, F. C. van den Bosch, A. Dekel, Mon. Not. R. Astron. Soc. 405, 1690 (2010).
25. N. Bouché et al., Astrophys. J. 718, 1001 (2010).
26. S. Genel et al., Astrophys. J. 688, 789 (2008).
27. J. McBride, O. Fakhouri, C. Ma, Mon. Not. R. Astron. Soc. 398, 1858 (2009).
28. M. Giavalisco et al., Astrophys. J. 743, 95 (2011).
29. K. H. R. Rubin, J. X. Prochaska, D. C. Koo, A. C. Phillips, Astrophys. J. 747, L26 (2012).
30. J. Ribaudo et al., Astrophys. J. 743, 207 (2011).

# A Population of Fast Radio Bursts at Cosmological Distances

D. Thornton,[1,2]* B. Stappers,[1] M. Bailes,[3,4] B. Barsdell,[3,4] S. Bates,[5] N. D. R. Bhat,[3,4,6] M. Burgay,[7] S. Burke-Spolaor,[8] D. J. Champion,[9] P. Coster,[2,3] N. D'Amico,[10,7] A. Jameson,[3,4] S. Johnston,[2] M. Keith,[2] M. Kramer,[9,1] L. Levin,[5] L. Milia,[7] C. Ng,[9] A. Possenti,[7] W. van Straten[3,4]

Searches for transient astrophysical sources often reveal unexpected classes of objects that are useful physical laboratories. In a recent survey for pulsars and fast transients, we have uncovered four millisecond-duration radio transients all more than 40° from the Galactic plane. The bursts' properties indicate that they are of celestial rather than terrestrial origin. Host galaxy and intergalactic medium models suggest that they have cosmological redshifts of 0.5 to 1 and distances of up to 3 gigaparsecs. No temporally coincident x- or gamma-ray signature was identified in association with the bursts. Characterization of the source population and identification of host galaxies offers an opportunity to determine the baryonic content of the universe.

The four fast radio bursts (FRBs) (Fig. 1) reported here were detected in the high Galactic latitude region of the High Time Resolution Universe (HTRU) survey (1), which was designed to detect short-time-scale radio transients and pulsars (Galactic pulsed radio sources). The survey uses the 64-m Parkes radio telescope and its 13-beam receiver to acquire data across a bandwidth of 400 MHz centered at 1.382 GHz (table S1). We measured minimum fluences for the FRBs of $F = 0.6$ to 8.0 Jy ms (1 Jy = $10^{-26}$ W m$^{-2}$ Hz$^{-1}$) (2). At cosmological distances, this indicates that they are more luminous than bursts from any known transient radio source (3). Follow-up observations at the original beam positions have not detected any repeat events,

indicating that the FRBs are likely cataclysmic in nature.

Candidate extragalactic bursts have previously been reported with varying degrees of plausibility (4–7), along with a suggestion that FRB 010724 (the "Lorimer burst") is similar to other signals that may be of local origin (8, 9). To be consistent with a celestial origin, FRBs should exhibit certain pulse properties. In particular, observations of radio pulsars in the Milky Way (MW) have confirmed that radio emission is delayed by propagation through the ionized interstellar medium (ISM), which can be considered a cold plasma. This delay has a power law dependence of $\delta t \propto DM \cdot \nu^{-2}$ and a typical frequency-dependent width of $W \propto \nu^{-4}$. The dispersion

measure (DM) is related to the integrated column density of free electrons along the line of sight to the source and is a proxy for distance. The frequency-dependent pulse broadening occurs as an astrophysical pulse is scattered by an inhomogeneous turbulent medium, causing a characteristic exponential tail. Parameterizing the frequency dependence of δt and W as α and β, respectively, we measured $\alpha = -2.003 \pm 0.006$ and $\beta = -4.0 \pm 0.4$ for FRB 110220 (Table 1 and Fig. 2), as expected for propagation through a cold plasma. Although FRB 110703 shows no evidence of scattering, we determined $\alpha = -2.000 \pm 0.006$. The other FRBs do not have sufficient

[1]Jodrell Bank Centre for Astrophysics, School of Physics and Astronomy, University of Manchester, Manchester M13 9PL, UK. [2]Commonwealth Science and Industrial Research Organisation (CSIRO) Astronomy and Space Science, Australia Telescope National Facility, Post Office Box 76, Epping, NSW 1710, Australia. [3]Centre for Astrophysics and Supercomputing, Swinburne University of Technology, Mail H30, Post Office Box 218, Hawthorn, VIC 3122, Australia. [4]Australian Research Council Centre of Excellence for All-Sky Astrophysics (CAASTRO), Mail H30, Post Office Box 218, Hawthorn, VIC 3122, Australia. [5]West Virginia University Center for Astrophysics, West Virginia University, Morgantown, WV 26506, USA. [6]International Centre for Radio Astronomy Research, Department of Imaging and Applied Physics, Faculty of Science and Engineering, Curtin University, Post Office Box U1987, Perth, WA 6845, Australia. [7]Istituto Nazionale di Astrofisica, Osservatorio Astronomico di Cagliari, Loc. Poggio dei Pini, Strada 54, 09012 Capoterra (CA), Italy. [8]Jet Propulsion Laboratory, California Institute of Technology, 4800 Oak Grove Drive, Pasadena, CA 91104, USA. [9]Max-Planck-Institut für Radio Astronomie, Auf dem Hugel 69, 53121 Bonn, Germany. [10]Dipartimento di Fisica, Universita di Cagliari, Cittadella Universitaria 09042, Monserrato (CA), Italy.

*Corresponding author. E-mail: thornton@jb.man.ac.uk

signal-to-noise ratios (SNRs) to yield astrophysically interesting constraints for either parameter and show no evidence of scattering.

Our FRBs were detected with DMs in the range from 553 to 1103 $cm^{-3}$ pc. Their high Galactic latitudes ($|b| > 41°$, Table 1) correspond to lines of sight through the low column density Galactic ISM corresponding to just 3 to 6% of the DM measured (10). These small Galactic DM contributions are highly supportive of an extragalactic origin and are substantially smaller fractions than those of previously reported bursts, which were 15% of DM = 375 $cm^{-3}$ pc for FRB 010724 (4) and 70% of DM = 746 $cm^{-3}$ pc for FRB 010621 (5).

The non-Galactic DM contribution, $DM_E$, is the sum of two components: the intergalactic medium (IGM; $DM_{IGM}$) and a possible host galaxy ($DM_{Host}$). The intervening medium could be purely intergalactic and could also include a contribution from an intervening galaxy. Two options are considered according to the proximity of the source to the center of a host galaxy.

If located at the center of a galaxy, this may be a highly dispersive region; for example, lines of sight passing through the central regions of Milky Way–like galaxies could lead to DMs in excess of 700 $cm^{-3}$ pc in the central ~100 pc (11), independent of the line-of-sight inclination. In this case, $DM_E$ is dominated by $DM_{Host}$ and requires FRBs to be emitted by an unknown mechanism in the central region, possibly associated with the supermassive black hole located there.

If outside a central region, then elliptical host galaxies (which are expected to have a low electron density) will not contribute to $DM_E$ substantially, and $DM_{Host}$ for a spiral galaxy will only contribute substantially to $DM_E$ if viewed close to edge-on [inclination, $i > 87°$ for DM > 700$cm^{-3}$pc; probability($i > 87°$) $\approx 0.05$]. The chance of all four FRBs coming from edge-on spiral galaxies is therefore negligible ($10^{-6}$). Consequently, if the sources are not located in a galactic center, $DM_{Host}$ would likely be small, and $DM_{IGM}$ dominates. Assuming an IGM free-electron distribution, which takes into account cosmological redshift and assumes a universal ionization fraction of 1 (12, 13), the sources are inferred to be at redshifts $z = 0.45$ to 0.96, corresponding to comoving distances of 1.7 to 3.2 Gpc (Table 1).

In principle, pulse scatter-broadening measurements can constrain the location and strength of an intervening scattering screen (14). FRBs 110627, 110703, and 120127 are too weak to enable the determination of any scattering; however, FRB 110220 exhibits an exponential scattering tail (Fig. 1). There are at least two possible sources and locations for the responsible scattering screens: a host galaxy or the IGM. It is possible that both contribute to varying degrees.

For screen-source, $D_{src}$, and screen-observer, $D_{obs}$, distances, the magnitude of the pulse broadening resulting from scattering is multiplied by the factor $D_{src}D_{obs}/(D_{src} + D_{obs})^2$. For a screen and source located in a distant galaxy, this effect

probably requires the source to be in a high-scattering region, for example, a galactic center.

The second possibility is scattering because of turbulence in the ionized IGM, unassociated with any galaxy. There is a weakly constrained empirical relationship between DM and measured scattering for pulsars in the MW. If applicable to the IGM, then the observed scattering implies $DM_{IGM} > 100cm^{-3}$ pc (2, 15). With use of the aforementioned model of the ionized IGM, this DM equates to $z > 0.11$ (2, 12, 13). The probability of an intervening galaxy located along the line of sight within $z \approx 1$ is $\leq 0.05$ (16). Such a galaxy could be a source of scattering and dispersion, but the magnitude would be subject to the same inclination dependence as described for a source located in the disk of a spiral galaxy.

It is important to be sure that FRBs are not a terrestrial source of interference. Observations at Parkes have previously shown swept frequency pulses of terrestrial origin, dubbed "perytons." These are symmetric $W > 20$ ms pulses, which imperfectly mimic a dispersive sweep (2, 8). Although perytons peak in apparent DM near 375 $cm^{-3}$ pc (range from ~200 to 420 $cm^{-3}$ pc),

close to that of FRB 010724, the FRBs presented here have much higher and randomly distributed DMs. Three of these FRBs are factors of >3 narrower than any documented peryton. Last, the characteristic scattering shape and strong dispersion delay adherence of FRB 110220 make a case for cold plasma propagation.

The Sun is known to emit frequency-swept radio bursts at 1 to 3 GHz [typeIIIdm (17)]. These bursts have typical widths of 0.2 to 10 s and positive frequency sweeps, entirely inconsistent with measurements of $W$ and $\alpha$ for the FRBs. Whereas FRB 110220 was separated from the Sun by 5.6°, FRB 110703 was detected at night and the others so far from the Sun that any solar radiation should have appeared in multiple beams. These FRBs were only detected in a single beam; it is therefore unlikely they are of solar origin.

Uncertainty in the true position of the FRBs within the frequency-dependent gain pattern of the telescope makes inferring a spectral index, and hence flux densities outside the observing band, difficult. A likely off-axis position changes the intrinsic spectral index substantially. The spectral
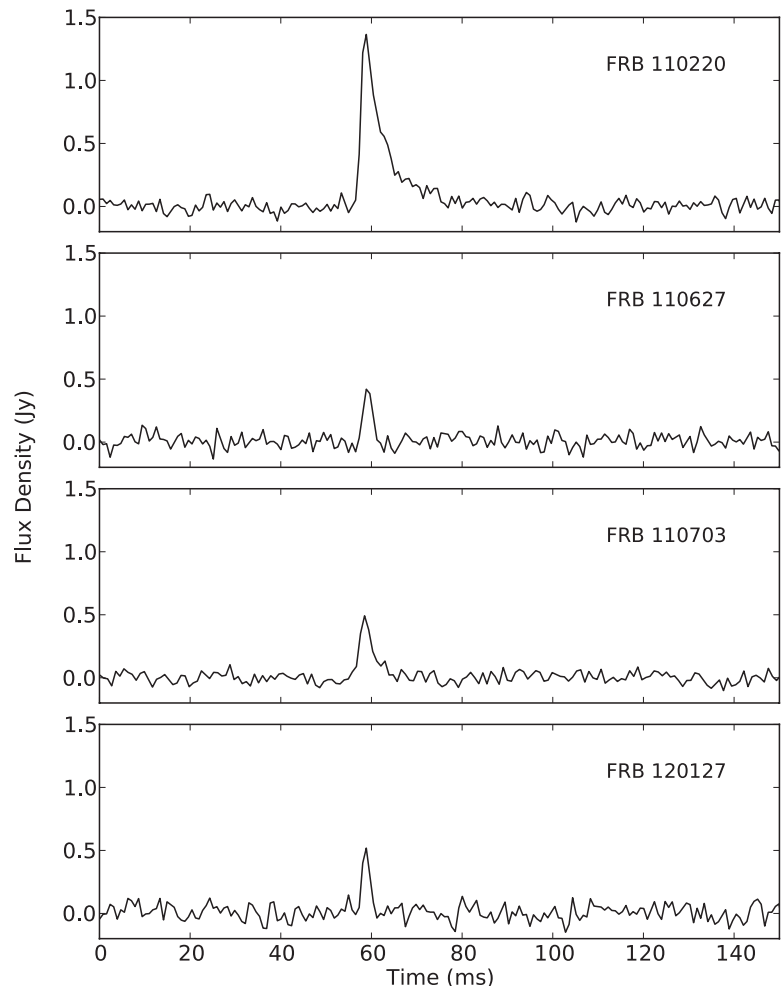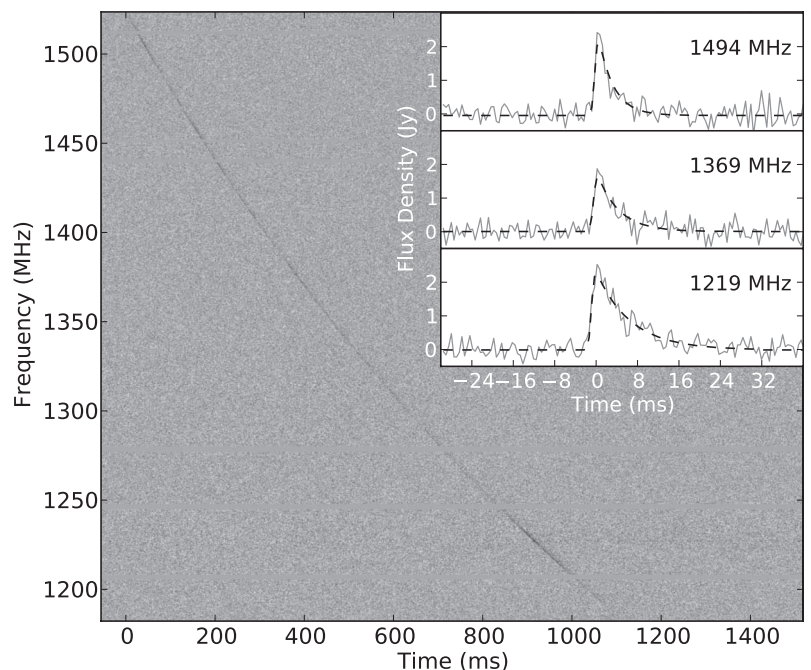


**Fig. 1. The frequency-integrated flux densities for the four FRBs.** The time resolutions match the level of dispersive smearing in the central frequency channel (0.8, 0.6, 0.9, and 0.5 ms, respectively).

**Table 1. Parameters for the four FRBs.** The position given is the center of the gain pattern of the beam in which the FRB was detected (half-power beam width ~ 14 arc min). The UTC corresponds to the arrival time at 1581.804688 MHz. The DM uncertainties depend not only on SNR but also on whether $\alpha$ and $\beta$ are assumed ($\alpha = -2$; no scattering) or fit for; where fitted, $\alpha$ and $\beta$ are given. The comoving distance was calculated by using $DM_{Host} = 100$ cm$^{-3}$ pc (in the rest frame of the host) and a standard, flat-universe $\Lambda$CDM cosmology, which describes the expansion of the universe with baryonic and dark matter and dark energy [$H_0 = 71$ km s$^{-1}$ Mpc$^{-1}$, $\Omega_M = 0.27$, $\Omega_\Lambda = 0.73$; $H_0$ is the Hubble constant and $\Omega_M$ and $\Omega_\Lambda$ are fractions of the critical density of matter and dark energy, respectively (29)]. $\alpha$ and $\beta$ are from a series of fits using intrinsic pulse widths of 0.87 to 3.5 ms; the uncertainties reflect the spread of values obtained (2). The observed widths are shown; FRBs 110627, 110703, and 120127 are limited by the temporal resolution due to dispersion smearing. The energy released is calculated for the observing band in the rest frame of the source (2).

|  | FRB 110220 | FRB 110627 | FRB 110703 | FRB 120127 |
|---|---|---|---|---|
| Beam right ascension (J2000) | 22$^h$ 34$^m$ | 21$^h$ 03$^m$ | 23$^h$ 30$^m$ | 23$^h$ 15$^m$ |
| Beam declination (J2000) | $-12°$ 24$'$ | $-44°$ 44$'$ | $-02°$ 52$'$ | $-18°$ 25$'$ |
| Galactic latitude, $b$ (°) | $-54.7$ | $-41.7$ | $-59.0$ | $-66.2$ |
| Galactic longitude, $l$ (°) | $+50.8$ | $+355.8$ | $+81.0$ | $+49.2$ |
| UTC (dd/mm/yyyy hh:mm:ss.sss) | 20/02/2011 01:55:48.957 | 27/06/2011 21:33:17.474 | 03/07/2011 18:59:40.591 | 27/01/2012 08:11:21.723 |
| DM (cm$^{-3}$ pc) | 944.38 ± 0.05 | 723.0 ± 0.3 | 1103.6 ± 0.7 | 553.3 ± 0.3 |
| DM$_E$ (cm$^{-3}$ pc) | 910 | 677 | 1072 | 521 |
| Redshift, $z$ (DM$_{Host}$ = 100 cm$^{-3}$ pc) | 0.81 | 0.61 | 0.96 | 0.45 |
| Co-moving distance, $D$ (Gpc) at $z$ | 2.8 | 2.2 | 3.2 | 1.7 |
| Dispersion index, $\alpha$ | $-2.003 ± 0.006$ | – | $-2.000 ± 0.006$ | – |
| Scattering index, $\beta$ | $-4.0 ± 0.4$ | – | – | – |
| Observed width at 1.3 GHz, $W$ (ms) | 5.6 ± 0.1 | <1.4 | <4.3 | <1.1 |
| SNR | 49 | 11 | 16 | 11 |
| Minimum peak flux density $S_\nu$ (Jy) | 1.3 | 0.4 | 0.5 | 0.5 |
| Fluence at 1.3 GHz, $F$ (Jy ms) | 8.0 | 0.7 | 1.8 | 0.6 |
| $S_\nu D^2$ (× 10$^{12}$ Jy kpc$^2$) | 10.2 | 1.9 | 5.1 | 1.4 |
| Energy released, $E$ (J) | ~10$^{33}$ | ~10$^{31}$ | ~10$^{32}$ | ~10$^{31}$ |

energy distribution across the band in FRB 110220 is characterized by bright bands ~100 MHz wide (Fig. 2); the SNRs are too low in the other three FRBs to quantify this behavior (2). Similar spectral characteristics are commonly observed in the emission of high-$|b|$ pulsars.

With four FRBs, it is possible to calculate an approximate event rate. The high-latitude HTRU survey region is 24% complete, resulting in 4500 square degrees observed for 270 s. This corresponds to an FRB rate of $R_{FRB}(F \sim 3$ Jy ms$) = 1.0^{+0.6}_{-0.5} \times 10^4$ sky$^{-1}$ day$^{-1}$, where the 1-$\sigma$ uncertainty assumes Poissonian statistics. The MW foreground would reduce this rate, with increased sky temperature, scattering, and dispersion for surveys close to the Galactic plane. In the absence of these conditions, our rate implies that $17^{+9}_{-7}$, $7^{+4}_{-3}$, and $12^{+6}_{-5}$ FRBs should be found in the completed high- and medium-latitude parts of the HTRU (1) and Parkes multibeam pulsar (PMPS) surveys (18).

One candidate FRB with DM > DM$_{MW}$ has been detected in the PMPS [$|b| < 5°$ (5, 19)]. This burst could be explained by neutron star emission, given a small scale-height error; however, observations have not detected any repetition. No excess-DM FRBs were detected in a burst search of the first 23% of the medium-latitude HTRU survey [$|b| < 15°$ (20)].

The event rate originally suggested for FRB 010724, $R_{010724} = 225$ sky$^{-1}$ day$^{-1}$ (4), is consistent with our event rate given a Euclidean universe and a population with distance-independent intrinsic luminosities (source count, $N \propto F^{-3/2}$) yielding $R_{FRB}$ ($F \sim 3$ Jy ms) $\sim 10^2 R_{FRB}(F_{010724} \sim 150$ Jy ms).

There are no known transients detected at gamma-ray, x-ray, or optical wavelengths or gravitational wave triggers that can be temporally associated with any FRBs. In particular there is

**Fig. 2. A dynamic spectrum showing the frequency-dependent delay of FRB 110220.** Time is measured relative to the time of arrival in the highest frequency channel. For clarity we have integrated 30 time samples, corresponding to the dispersion smearing in the lowest frequency channel. (**Inset**) The top, middle, and bottom 25-MHz-wide dedispersed subband used in the pulse-fitting analysis (2); the peaks of the pulses are aligned to time = 0. The data are shown as solid gray lines and the best-fit profiles by dashed black lines.

no known gamma-ray burst (GRB) with a coincident position on a time scale commensurate with previous tentative detections of short-duration radio emission (6). GRBs have highly beamed gamma-ray emission (21), and, if FRBs are associated with them, the radio emission must be beamed differently. By using the distances in Table 1, we found that the comoving volume contains $\sim 10^9$ late-type galaxies (22), and the FRB rate is therefore $R_{FRB} \sim 10^{-3}$ year$^{-1}$ per galaxy. $R_{FRB}$ is thus inconsistent with $R_{GRB} \sim 10^{-6}$ year$^{-1}$ per galaxy, even when beaming of emission is accounted for (21). Soft gamma-ray repeaters (SGRs) undergo giant bursts at a rate consistent with FRBs (23), and the energy within our band is well within the budget of the few known SGR giant burst cases (24).

Another postulated source class is the interaction of the magnetic fields of two coalescing neutron stars (25). However, the large implied FRB luminosities indicate that coalescing neutron stars may not be responsible for FRBs. Furthermore, $R_{FRB}$ is substantially higher than the predicted rate for neutron star mergers. Black hole evaporation has also been postulated as a source of FRBs; however, the predicted luminosity within our observing band far exceeds the energy budget of an evaporation event (26).

The core-collapse supernova (ccSN) rate of $R_{ccSN} \sim 10^{-2}$ year$^{-1}$ per galaxy (27) is consistent with $R_{FRB}$. There is no known mechanism to generate an FRB from a lone ccSN. It may, however, be possible that a ccSN with an orbiting neutron star can produce millisecond-duration radio bursts during the interaction of the ccSN explosion and the magnetic field of the neutron star (28), although the need for an orbiting neutron star will make these rarer.

As extragalactic sources, FRBs represent a probe of the ionized IGM. Real-time detections and immediate follow-up at other wavelengths may identify a host galaxy with an independent redshift measurement, thus enabling the IGM baryon content to be determined (12). Even without host identifications, further bright FRB detections will be a unique probe of the magneto-ionic properties of the IGM.

### References and Notes

1. M. J. Keith et al., *Mon. Not. R. Astron. Soc.* **409**, 619–627 (2010).
2. Materials and methods are available as supplementary materials on *Science* Online.
3. J. M. Cordes, *SKA Memo Ser.* **97**, 1 (2009).
4. D. R. Lorimer et al., *Science* **318**, 777–780 (2007); 10.1126/science.1147532.
5. E. F. Keane, B. W. Stappers, M. Kramer, A. G. Lyne, *Mon. Not. R. Astron. Soc.* **425**, L71–L75 (2012).
6. K. W. Bannister, T. Murphy, B. M. Gaensler, J. E. Reynolds, *Astrophys. J.* **757**, 38 (2012).
7. E. Rubio-Herrera, B. W. Stappers, J. W. T. Hessels, R. Braun, *Mon. Not. R. Astron. Soc.* **428**, 2857–2873 (2013).
8. S. Burke-Spolaor et al., *Astrophys. J.* **727**, 18 (2011).
9. The Lorimer burst is designated as FRB 010724; this date is a correction to that in the original paper.
10. J. M. Cordes, T. J. W. Lazio (2002), http://arxiv.org/abs/astroph/0207156.
11. J. S. Deneva, J. M. Cordes, T. J. W. Lazio, *Astrophys. J.* **702**, L177–L181 (2009).
12. K. Ioka, *Astrophys. J.* **598**, L79–L82 (2003).
13. S. Inoue, *Mon. Not. R. Astron. Soc.* **348**, 999–1008 (2004).
14. I. P. Williamson, *Mon. Not. R. Astron. Soc.* **157**, 55 (1972).
15. N. D. R. Bhat et al., *Astrophys. J.* **605**, 759–783 (2004).
16. R. C. Roeder, R. T. Verreault, *Astrophys. J.* **155**, 1047 (1969).
17. H. Isliker, A. O. Benz, *Astron. Astrophys. Suppl. Ser.* **104**, 145 (1994).
18. R. N. Manchester et al., *Mon. Not. R. Astron. Soc.* **328**, 17–35 (2001).
19. M. Bagchi, A. C. Nieves, M. McLaughlin, *Mon. Not. R. Astron. Soc.* **425**, 2501–2506 (2012).
20. S. Burke-Spolaor et al., *Mon. Not. R. Astron. Soc.* **416**, 2465–2476 (2011).
21. D. A. Frail et al., *Astrophys. J.* **562**, L55–L58 (2001).
22. D. S. Madgwick et al., *Mon. Not. R. Astron. Soc.* **333**, 133–144 (2002).
23. E. O. Ofek, *Astrophys. J.* **659**, 339–346 (2007).
24. K. Hurley et al., *Nature* **434**, 1098–1103 (2005).
25. B. M. S. Hansen, M. Lyutikov, *Mon. Not. R. Astron. Soc.* **322**, 695–701 (2001).
26. M. J. Rees, *Nature* **266**, 333–334 (1977).
27. R. Diehl et al., *Nature* **439**, 45–47 (2006).
28. A. E. Egorov, K. A. Postnov, *Astron. Lett.* **35**, 241–246 (2009).
29. N. Spergel et al., *Astrophys. J. Suppl. Ser.* **148**, 175–194 (2003).

# Ultrafast Three-Dimensional Imaging of Lattice Dynamics in Individual Gold Nanocrystals

J. N. Clark,[1]* L. Beitra,[1] G. Xiong,[1] A. Higginbotham,[2] D. M. Fritz,[3] H. T. Lemke,[3] D. Zhu,[3] M. Chollet,[3] G. J. Williams,[3] M. Messerschmidt,[3] B. Abbey,[4] R. J. Harder,[5] A. M. Korsunsky,[6,7] J. S. Wark,[2] I. K. Robinson[1,7]

Key insights into the behavior of materials can be gained by observing their structure as they undergo lattice distortion. Laser pulses on the femtosecond time scale can be used to induce disorder in a "pump-probe" experiment with the ensuing transients being probed stroboscopically with femtosecond pulses of visible light, x-rays, or electrons. Here we report three-dimensional imaging of the generation and subsequent evolution of coherent acoustic phonons on the picosecond time scale within a single gold nanocrystal by means of an x-ray free-electron laser, providing insights into the physics of this phenomenon. Our results allow comparison and confirmation of predictive models based on continuum elasticity theory and molecular dynamics simulations.

Coherent lattice vibrations (phonons) in solids play an important role in many phenomena such as melting (1–5), phase transitions (6), bond softening (7) and hardening (8), and ferroelectricity (9). Ultrashort (femtosecond) laser pulses have been used to reveal great detail about the dynamics of these phenomena; however, many of these studies have been confined to bulk samples or ensembles of nanoparticles. With nanoparticles playing an increasingly important role in technology, from catalysis (10) and photonic devices (11) to single-particle mass spectrometry (12) and sensing, understanding the mechanical and dynamical properties of single nanoparticles becomes very important as many of the processes occur on femtosecond (fs) and picosecond (ps) time scales.

The characterization of lattice displacements in individual nanoparticles over very short time scales with atomic sensitivity has been challenging. The interrogation of individual particles is important, as ensemble heterogeneity can give the

[1]London Centre for Nanotechnology, University College London, London WC1E 6BT, UK. [2]Department of Physics, Clarendon Laboratory, University of Oxford, Parks Road, Oxford OX1 3PU, UK. [3]Linac Coherent Light Source, SLAC National Accelerator Laboratory, 2575 Sand Hill Road, Menlo Park, CA 94025, USA. [4]ARC Centre of Excellence for Coherent X-ray Science, Department of Physics, La Trobe University, Bundoora, Victoria 3086, Australia. [5]Advanced Photon Source, Argonne, IL 60439, USA. [6]Department of Engineering Science, University of Oxford, Parks Road, Oxford OX1 3PJ, UK. [7]Research Complex at Harwell, Didcot, Oxfordshire OX11 0DE, UK.

*Corresponding author. E-mail: jesse.clark@ucl.ac.uk
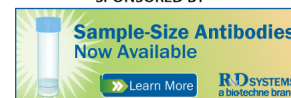
# A Population of Fast Radio Bursts at Cosmological Distances

D. Thornton *et al.*

Science
AAAS